MICROCOPY RESOLUTION TEST CHART

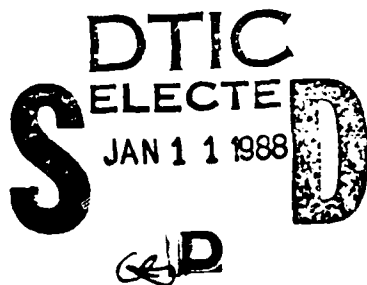NATIONAL BUREAU OF STANDARDS 1963 A

Naval Research Laboratory

DTIC FILE COPY

High-Current Density, High-Brightness Electron Beams from Large-Area Lanthanum Hexaboride Cathodes*

P. LOSCHIALPO AND C.A. KAPETANAKOS

*Advanced Beam Technologies Branch
Plasma Physics Division*

AD-A187 700

DTIC
SELECTED
JAN 1 1 1988
D

December 13, 1987

REPORT DOCUMENTATION PAGE

Form Approved
OMB No 0704-0188

1a. REPORT SECURITY CLASSIFICATION UNCLASSIFIED	1b. RESTRICTIVE MARKINGS *AI87770*
2a. SECURITY CLASSIFICATION AUTHORITY	3 DISTRIBUTION/AVAILABILITY OF REPORT
2b. DECLASSIFICATION/DOWNGRADING SCHEDULE	Approved for public release; distribution unlimited.

4. PERFORMING ORGANIZATION REPORT NUMBER(S) NRL Memorandum Report 6119	5. MONITORING ORGANIZATION REPORT NUMBER(S)

6a. NAME OF PERFORMING ORGANIZATION Naval Research Laboratory	6b. OFFICE SYMBOL (If applicable)	7a. NAME OF MONITORING ORGANIZATION

6c. ADDRESS (City, State, and ZIP Code) Washington, DC 20375-5000	7b. ADDRESS (City, State, and ZIP Code)

8a. NAME OF FUNDING/SPONSORING ORGANIZATION Office of Naval Research	8b. OFFICE SYMBOL (If applicable)	9 PROCUREMENT INSTRUMENT IDENTIFICATION NUMBER

8c. ADDRESS (City, State, and ZIP Code) 800 North Quincy Street Arlington, VA 22217	10 SOURCE OF FUNDING NUMBERS			
	PROGRAM ELEMENT NO. 61153	PROJECT NO	TASK NO RR011-09-41	WORK UNIT ACCESSION NO

11. TITLE (Include Security Classification)

High-Current Density, High-Brightness Electron Beams from Large-Area Lanthanum Hexaboride Cathodes*

12. PERSONAL AUTHOR(S)
Loschialpo, P. and Kapetanakos, C.A.

13a. TYPE OF REPORT Interim	13b. TIME COVERED FROM _____ TO _____	14. DATE OF REPORT (Year, Month, Day) 1987 December 13	15 PAGE COUNT 34

16. SUPPLEMENTARY NOTATION

*Supported partially by DARPA and partially by ONR.

17. COSATI CODES			18. SUBJECT TERMS (Continue on reverse if necessary and identify by block number)
FIELD	GROUP	SUB-GROUP	Beam quality Brightness
			Cathodes

19. ABSTRACT (Continue on reverse if necessary and identify by block number)

Large ($\neq$ 5 cm) diameter lanthanum hexaboride (LaB$_6$) cathodes operated at 10 kV have produced 1-5 μs electron pulses with current density between 10 and 20 A/cm^2. Normalized beam brightness, $B_n = I/(\pi \beta \gamma \epsilon)^2$, approximately 3×10^5 A/cm^2 –rad^2 has been consistently measured. To obtain this high current density, the LaB$_6$ cathodes have been heated to temperatures between $\sim 1600 - 1800°$C. Very uniform temperature profiles are obtained by applying a carefully tailored electron bombardment heating power distribution. These measurements have been made between pressure 10^{-6} to 10^{-5} Torr, i.e., under much less demanding vacuum conditions than that required by conventional dispenser type cathodes.

20 DISTRIBUTION/AVAILABILITY OF ABSTRACT ☒ UNCLASSIFIED/UNLIMITED ☐ SAME AS RPT ☐ DTIC USERS	21 ABSTRACT SECURITY CLASSIFICATION UNCLASSIFIED
22a. NAME OF RESPONSIBLE INDIVIDUAL P. Loschialpo	22b TELEPHONE (Include Area Code) 22c OFFICE SYMBOL

DD Form 1473, JUN 86   Previous editions are obsolete.   SECURITY CLASSIFICATION OF THIS PAGE

S/N 0102-LF-014-6603

i

CONTENTS

A-1

iii

HIGH-CURRENT DENSITY, HIGH-BRIGHTNESS ELECTRON BEAMS FROM LARGE-AREA LANTHANUM HEXABORIDE CATHODES*

I. INTRODUCTION

There is a growing demand for cathodes that are capable of generating high current density, high quality electron beam pulses with high repetition rate. Such cathodes have application in several high power, short wavelength devices that intend to produce C.W. coherent radiation, including gyrotrons[1,2] and Free Electron Lasers[2,3] (FELs).

In the past, several free electron laser experiments used cold electron cathodes, such as plasma cathodes, graphite brush cathodes, or velvet cathodes.[4-6] However, these sources are not suitable for repetitively pulsed devices. Conventional thermionic dispenser-type cathodes are capable of producing high frequency, repetitively pulsed beams, but are limited to 1-4 A/cm^2. More recent work with chemically depositing osmium coatings have resulted in a large increase in emission (40-50 A/cm^2).[7] However, this important development is limited to application in devices where ultra-high vacuum is maintained.

Lanthanum hexaboride (LaB_6) is of interest as a thermionic cathode because of its ability to produce high current density electron beam pulses (10-50 A/cm^2) with high repetition rate, while requiring only modest vacuum on the order of 10^{-5} Torr.[8-10] For example, Gallagher reported that LaB_6 cathodes at a temperature of 1400°C are resistant to poisoning for air pressure as high as 5 X 10^{-5} Torr. He also reported that resistance to poisoning increases with increasing temperature.

Most of the previous work with LaB_6 has been limited to cathode cross sections < 1 mm diameter. High-power free electron lasers require large currents. Therefore an experimental study of large LaB_6 cathodes and their emission properties is needed.

A technique to uniformly heat large LaB_6 cathodes to 1600° - 1800°C, required for high current density emission, is first presented. This is followed by a brief description of the diagnostics used in this experiment. Cathode temperature profiles are shown which demonstrate the ability to achieve a uniform temperature distribution over a large area. Current measurements as a function of voltage are also presented. Results from emittance measurements are then described which permit a determination of normalized beam brightness. This result is compared with analytical calculations of emittance due to cathode temperature and surface roughness.

II. DESCRIPTION OF EXPERIMENT

A. Cathode heating.

The cathodes used are 5 cm diameter, 0.6 cm thick planar discs formed by hot pressing of LaB_6 powder. These sintered discs are commercially available at densities 70% to 90% of the solid LaB_6 density of 4.72 g/cm^3. Special tooling is required to machine this material, which has ceramic-like hardness, in order to mount the cathodes in a support structure. These cathodes must be heated to very high temperatures in order to obtain high current density electron emission. This is due to the material's high work function.

The thermionic limited electron current density is determined by the Richardson-Dushman equation:

$$J(A/cm^2) = AT^2 e^{-(11600\phi/T)} , \tag{1}$$

where A and ϕ are constants and T is the cathode temperature in degrees Kelvin. Lafferty[8] has reported the values 29 A/cm^2 - $^{\circ}$K^2 and 2.66 eV for A and ϕ respectively. Field assisted thermionic emission is determined by

$$J(A/cm^2) = AT^2 e^{[(139\ \varepsilon^{1/2}/T)-(11600\ \phi/T)]}, \qquad (2)$$

where ε is the electric field at the surface of the cathode in kV/cm. Equation (2) is known as the Schottky equation. Both Eqs. (1) and (2) are plotted in Fig. (1) as a function of cathode temperature in degrees Celsius. This figure shows that in order to obtain current density emission of 10 to 50 A/cm^2 the cathode surface must be heated between 1600 - 1800°C. For uniform current density emission, the entire surface of the cathode should be heated uniformly.

In the present experiment a uniform temperature profile was achieved over the cathode's emitting surface with the help of MITAS, a computer thermal analysis code developed by Martin Marietta Corporation. MITAS includes radiation and conduction as well as the geometrical details of the cathode assembly and the anode. The code results were useful in the selection of materials and fabrication techniques for the different parts of the cathode heater assembly. The results also provide the heat loss profile of the cathode. Figure 2 shows the cathode temperature profile for a specific applied power density distribution. It is apparent that heat is lost predominantly from the edge of the cathode due to thermal radiation. Therefore, the cathode heater assembly was designed to preferentially heat the cathode toward its edges to achieve a uniform temperature distribution.

A schematic of the cathode heater assembly is shown in Figure 3. The cathode is mounted in a graphite hollow disc. Graphite is chosen because it is known not to react with LaB$_6$.[8] The graphite disc is supported by a 0.1 mm thick tantalum cylindrical shell, which also serves as a radial heat shield. Two additional radial heat shields are included in the design. The intermediate heat shield supports a thin annular graphite hollow disc.

which is positioned flush with the cathode surface to serve as an electric field shaper. In addition, four tantalum plates are used as axial heat shields. Directly behind the cathode, a 0.5 mm diameter tungsten filament is woven into a circular disc of boron nitride, which serves as a filament support. After experimenting with different tungsten alloys (pure W and 1% Th-W), we have selected a 3% Re-W alloy that is less brittle and easier to wind than the other alloys tested.

The LaB$_6$ cathode is radiantly warmed from room temperature to 1000°C by passing 0 to 16 A through the filament. Additional heater power is provided by electron bombardment to raise the cathode temperature from 1000°C to the desired operating value (~1600° to 1800°C). Typically the filament is held at -700 V potential with respect to the cathode. Electrons emitted from the hot filament are accelerated toward the cathode where their energy is deposited as heat. After an initial "burn-in" period, the boron-nitride filament support base becomes coated with a purple colored film, which is LaB$_6$ evaporated from the cathode.[10] This film enhances the electron bombardment current, which finally saturates at an upper limit. This limit is the same as the space-charge limited current for electrons emitted from the entire filament support base surface for the specific filament base to cathode distance. The bombardment current limit is typically 3 to 4 A. During operation the pressure was between 10^{-6} to 10^{-5} Torr.

The space-charge limited bombardment current was very stable. As a result, it was easy to hold the cathode temperature constant in time to ±10°C during operation.

The space-charge limited bombardment current density[11] is given by

$$J(A/cm^2) = 2.336 \times 10^{-6} V^{3/2}/D^2, \tag{3}$$

where V is the filament-cathode potential in Volts and D is the distance in cm between the cathode and filament support base. The heat deposition

profile is controlled by making D larger in the center than near the edge of the cathode. As a consequence, the edge of the cathode receives more current and therefore more power than the cathode center, resulting in a nearly uniform cathode temperature profile. Variation of D is accomplished by machining the filament base to a depth determined with the aid of the MITAS code. In the experiment, D at the center of the cathode was approximately 50% larger (0.9 cm) than at the edge (0.6 cm).

B. Diagnostics

A flat planar anode is positioned parallel with the cathode. This is shown schematically in Fig. 4. The anode is mounted to an X, Y, Z manipulator, allowing one to vary the anode-cathode gap and the two transverse coordinates of the anode (X, Y) during the experiment. The flat anode surface is made of 1 mm thick tantalum.

The temperature of the cathode is measured using a Land Instruments infrared thermometer, which detects thermal radiation from 0.8 to 1.1 μm. The resolution of the instrument is ±1°C. Temperature readings are corrected for spectral emissivity, using the value of 0.82, and for absorption by the glass viewport.[12, 13]

A 5 mm diameter hole has been drilled in the anode at 1.3 cm from the anode center. This hole allows the temperature to be measured by focusing the infrared thermometer on the cathode surface. Cathode temperature profiles at different fixed X positions are made by synchronously scanning the anode and infrared thermometer in the Y direction.

With the cathode at the desired operating temperature, a beam is generated by applying a negative 1 to 10 kV pulse to the cathode with respect to the grounded anode. The pulse width is 3 to 6 μs long, measured

5

from pulse initiation to the end of the voltage flat top, and is continuously variable. Voltage pulses are created by discharging a capacitor through the cathode-anode load. A Tektronix voltage probe measures the voltage amplitude, which is consistent with the known potential that the capacitor is charged to. Cathode emission current is measured with a Rogowski coil.

Emittance is measured by employing a 50 μm diameter pinhole drilled in a 130 μm thick sheet of tantalum foil. This foil is spot welded over another 5 mm diameter hole in the anode tantalum plate 1.3 cm off center, opposite from the temperature measuring hole. The setup is shown in Fig. 4. A beamlet emerging from the pinhole travels a drift length L of 15 cm and strikes a phosphor coated stainless steel plate. The normal of the phosphor plate surface is tilted 45° with respect to the beam axis of symmetry so that the beamlet image can be photographed. The beamlet image is much larger than the pinhole size. The angular divergence of the beamlet, θ, is then ΔY/L, where ΔY is the half width of the beamlet image in the Y-direction. Photographs of the beamlet are made at different cathode positions by scanning the anode in the Y direction. Spacial dimensions of the beamlet photographs are measured by raster scanning the photographs with an optical densitometer. The full width projected on the Y-axis, 2ΔY, is determined for each beamlet and from this an average value of ΔY for all the beamlets is computed. ΔY is experimentally observed to be substantially invariant of both number of photographic shots and pulse width. Typically, 20 shots are superimposed to get a clear photographic image of each beamlet. An average value, $\bar{\theta}$, of θ is determined. The normalized emittance[14, 15], ε_n, is then evaluated from

$$\varepsilon_n = \beta\gamma R_c \bar{\theta}, \qquad (4)$$

where R_c is the radius of the cathode emitting surface and β and γ are the usual relativistic factors. The pinhole size and 15 cm drift distance have been carefully chosen so that space charge expansion of the beamlet can be neglected. Divergence due to electrostatic deflection of the pinhole is also negligible. The normalized brightness of the beam is determined from

$$B_n = I_c/(\pi \, \varepsilon_n)^2, \tag{5}$$

where I_c is the cathode emission current.

III. RESULTS

A. Cathode temperature measurements

As discussed in section II, temperature-limited current density increases rapidly with temperature. This makes high temperature operation desirable. The highest cathode temperature measured in our experiment is 1781°C. Limitations to achieving higher temperatures include electron bombardment power supply current limits and, to a lesser extent, power radiated from the cathode heater assembly, which heats the vacuum chamber walls and causes excessive outgassing. Also, for temperatures much above 1800°C evaporation from the cathode surface becomes excessive.[8] The cathode is routinely operated at temperatures up to 1700°C.

Figure 5 illustrates the D.C. power levels required to heat the 5 cm diameter cathode to a given temperature. Up to 1000°C the cathode is heated by radiant power due to the filament current. Above 1000°C both electron bombardment and radiant power contribute to the cathode heating. The total power shown in Fig. 5 is the sum of bombardment power and radiant power. As temperature increases above 1000°C the supplied bombardment power increases steadily and becomes larger than the radiant power above 1400°C. Upwards of 1600°C the filament radiant power is only a small

fraction of the bombardment power.   Often the filament current is reduced
at this point to increase the filament's lifetime.

Figure 6 shows an example of a measured temperature profile. The
cathode is scanned in the Y direction for different X positions. Both X
and Y are measured from the center of the cathode. Data, represented by
the discrete open circles, are connected by straight line segments. The
cathode temperature is uniform to $\pm 20°C$. Additional modification of the
filament support base to concentrate more heat on the cathode edge may
improve uniformity even further.

B. Cathode current measurements

Cathode currents are measured for different cathode-anode potentials
and gap sizes.   Currents as high as 200 A are routinely measured,
corresponding to an average current density of 12 A/cm^2 over the 16 cm^2
cathode emitting area.

Figure 7 shows a plot of measured cathode current as a function of
cathode voltage for two different anode-cathode gaps, D. The measured data
are represented by either open circles or open squares. Data in this
figure are for a cathode temperature of 1600°C. Also shown in the graph
are solid lines of constant perveance.   These solid lines are calculated
from Child's law, Eq. (3), for D = 0.3, 0.4, and 0.5 cm, using an emitting
area of 16 cm^2. It is clear from Fig. 7 that the data closely follow the
corresponding constant perveance lines within the experimental uncertainty.
This indicates that the beam is space-charge limited.   The primary
experimental uncertainty is the size of the cathode-anode gap. In general,
more current is observed than that predicted by the field-assisted
thermionic emission. Specifically, for D = 0.4 cm, V = 9.0 kV and T =
1600°C, Eq. (2) gives 170 A, which is approximately 85% of the measured

8

current. This may be due to ions knocked off the anode by the primary electron beam. These ions would be accelerated toward the cathode where they in turn produce secondary electrons which add to the primary beam current. Another possibility is that the values of work function, ϕ, and Richardson constant, A, are significantly different than Lafferty's values of 2.66 eV and 29 A/cm^2-°K^2 used in determining the graph in Fig. 1. For example, Ahmed reported ϕ = 2.4 eV and A = 40 A/cm^2 - °K^2.[10] This can also account for the difference between the observed current and the computed temperature limited current.

C. Beam brightness measurements

Brightness is a useful measure of beam quality for FEL experiments.[16] Brightness, as previously discussed, is experimentally determined by measuring the normalized beam emittance and cathode emission current. Then brightness is readily computed using Eq. (5).

Results reported in the paper are for a cathode temperature of 1560°C. Higher cathode temperatures cause excess background light on the phosphor plate. Beam energy and current are 10 keV and 85 A respectively. The cathode-anode gap is measured to be 0.5 cm. During these measurements the pinhole was located, in succesive runs, at Y = 0.0, 0.5 and 1.0 cm from the cathode midplane and was displaced from the vertical axis that passes through the cathode center by 1.3 cm. At each Y position θ is determined. From these values of θ, the average angular divergence is computed to be

$\bar{\theta}$ = 11±2 mrad. Then, from Eqs. (4) and (5), ε_n = 5.0±1 cm-mrad and the normalized brightness is B$_n$ = 3.4±1 X 10^5 A/cm^2-rad^2.

Effects that may contribute to the observed emittance include the cathode temperature, non uniform emission and surface roughness. The

cathode temperature imposes a lower bound on the emittance of a beam emitted from a thermionic cathode. For a uniform temperature and emission profile, normalized RMS emittance due to temperature is given approximately by $\varepsilon_T = \beta\gamma R_c(2kT/eV)^{1/2}$, where k is Boltzmann's constant, T is the absolute temperature, and eV is the beam energy at the anode.[14] From this equation, ε_T = 2.6 cm-mrad for a 10 keV beam of electrons emitted from a 5 cm diameter cathode operated at 1560°C.

Contribution to the emittance from non uniform emission at the cathode is not probably very important, because the transit time of the electrons is substantially shorter than the electron plasma period, at least for the temperature limited case. Figure 8 shows electron microscope photographs of LaB$_6$ cathodes before use and after 28 hours of use at the operating temperature of 1550°C or higher. It is apparent that these cathodes are initially rather smooth and have only slowly varying surface irregularities. During operation the cathode surface becomes much rougher. Protrusions and craters appear scattered over the cathode surface. To what extent the roughness is caused by cathode heating alone and to to what extent the roughness is caused by electron beam operation is presently uncertain. One possible mechanism is that ions knocked off the anode surface by the incident electron beam are subsequently accelerated back to the cathode surface and their impact creates the observed roughness features. The height of the cathode protrusions vary between 0 and 4 µm, with a median value of 2 µm. Y.Y. Lau has derived analytic equations which enable one to calculate the emittance that is due to surface roughness as a function of height, h, and width, w, of the protrusions.[17] For our experimental parameters, V = 10 kV and D = 0.5 cm, ε_n varies only about ±10% for w/h varying over the range from 0 to 1. The median value of ε_n,

for $h = 2$ μm and w/h between 0 and 1, is then 1.9 cm-mrad for space-charge limited emission and 6.3 cm-mrad for temperature-limited emission. The experimental value, $\varepsilon_n = 5.0 \pm 1$ cm-mrad, is measured for the transitional region between space charge and temperature limited emission. The roughness contribution to ε_n, which falls between 1.9 cm-mrad and 6.3 cm-mrad is then consistent with our measured value.

IV. CONCLUSIONS

This paper reports on the generation of high current density, high brightness, long duration electron beam pulses from large area $L_a B_6$ cathodes. These measurements have been made between pressure 10^{-6} to 10^{-5} Torr, i.e., under substantially less demanding vacuum conditions than that required by conventional dispenser type cathodes.

Our results indicate that $L_a B_6$ cathodes have substantial potential in the generation of coherent radiation in repetitively pulsed devices or in the generation of long pulse duration radiation. Their resistance to poisoning make them more attractive than other thermionic cathodes but their high temperature requires special care in the design of the gun and the selection of its components.

REFERENCES

1. See for example: Special Issue on Gyrotrons, Intern. Journal of Electr. 57, No. 6. (1984).

2. P. Sprangle and T. Coffey, Physics Today, March 1984.

3. P. Sprangle, Robert A. Smith, and V.L. Granatstein, in Infrared and Millimeter Waves-Sources of Radiation, edited by Kenneth J. Button (Academic, New York, 1979), Vol. 1, p. 279.

4. J.A. Pasour, R.F. Lucey, C.W. Roberson in Free Electron Generators of Coherent Radiation, edited by C.A. Brau, S.F. Jacobs, and M.O. Scully, SPIE Conference Proceedings (SPIE, Bellingham, Wash. 1984) Vol. 453, pp. 328-335.

5. Juan J. Ramirez and Donald L. Cook, J. Appl. Phys. 51, 4602 (1980).

6. J.T. Weir, G.J. Caporaso, F.W. Chambers, R. Kalibjian, J. Kallman, D.S.Prono, M.E. Slominski, and A.C. Paul, IEEE Trans. Nucl. Sci. NS-32, 1812 (1985).

7. Arnold Shih, Alan Berry, Christie R.K. Marrian, and George A. Haas, IEEE Trans. Elec. Dev. ED-34, 1193 (1987).

8. J.M. Lafferty, J. Appl. Phys. 22, 299 (1951).

9. H.E. Gallagher, J. Appl. Phys. 40, 44 (1969).

10. H. Ahmed and A.N. Broers, J. Appl. Phys. 43, 2185 (1972).

11. C.D. Child, Phys. Rev. 32, 492 (1911).

12. V.S. Fomenko, Yu. B. Paderno, G.V. Samsonov, Ogneoupory 27, 40 (1962).

13. G.V. Samsonov, Hand Book of High Temperature Materials (Plenum, New York, 1964), Vol. 2, p. 169.

14. J.D. Lawson, The Physics of Charged-Particle Beams (Clarendon, Oxford, 1977), Chaps. 4.3-4.4.

15. Claude Lejeune and Jean Aubert, in Applied Charged Particle Optics, edited by A. Septier (Academic, New York, 1980), Part A, p. 159.

16. Thomas C. Marshall, Free-Electron Lasers (Macmillan, New York, 1985), pp. 103-104.

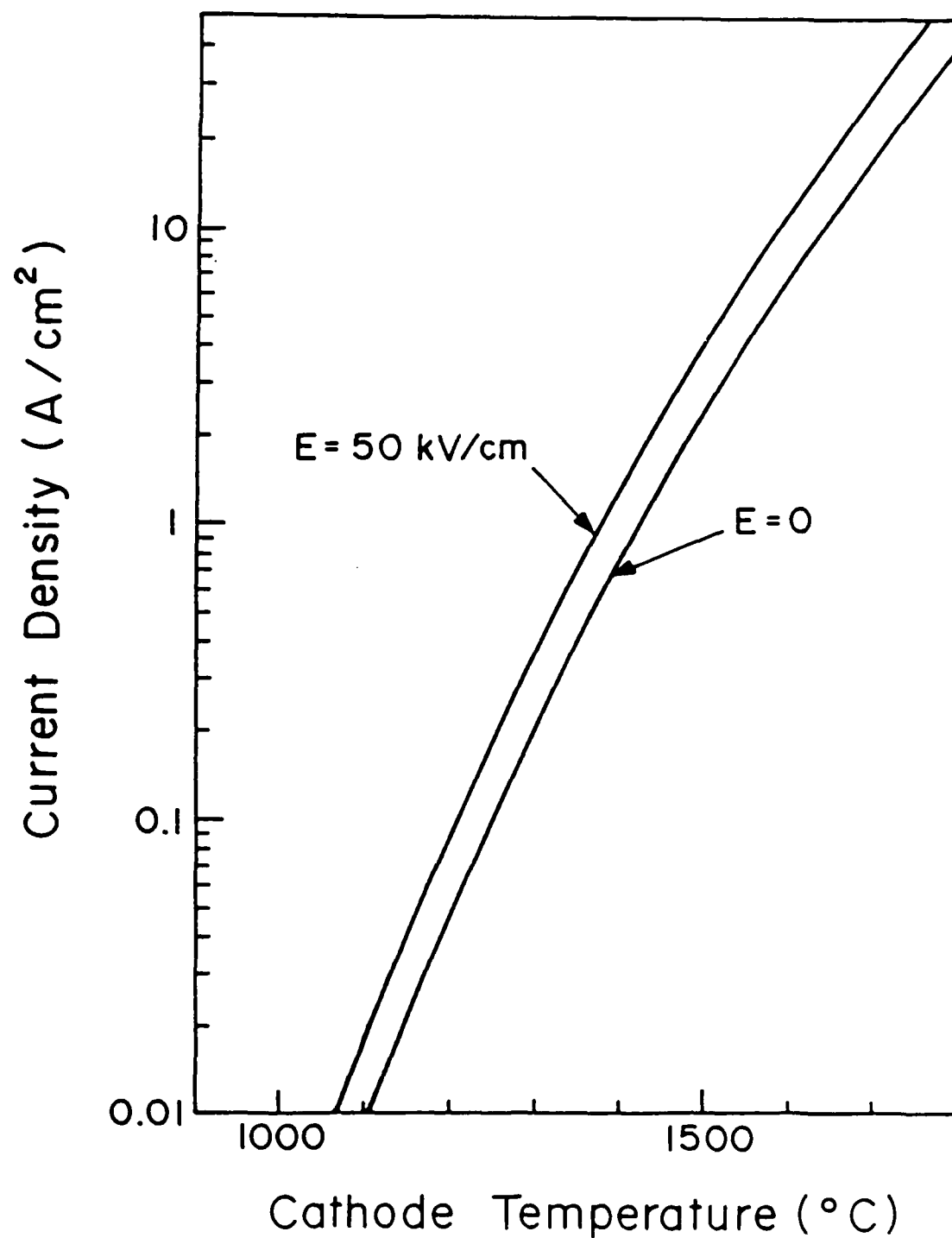17. Y.Y. Lau, J. Appl. Phys. 61, 36 (1987).

Fig. 1 — Temperature limited current density calculated for zero electric field
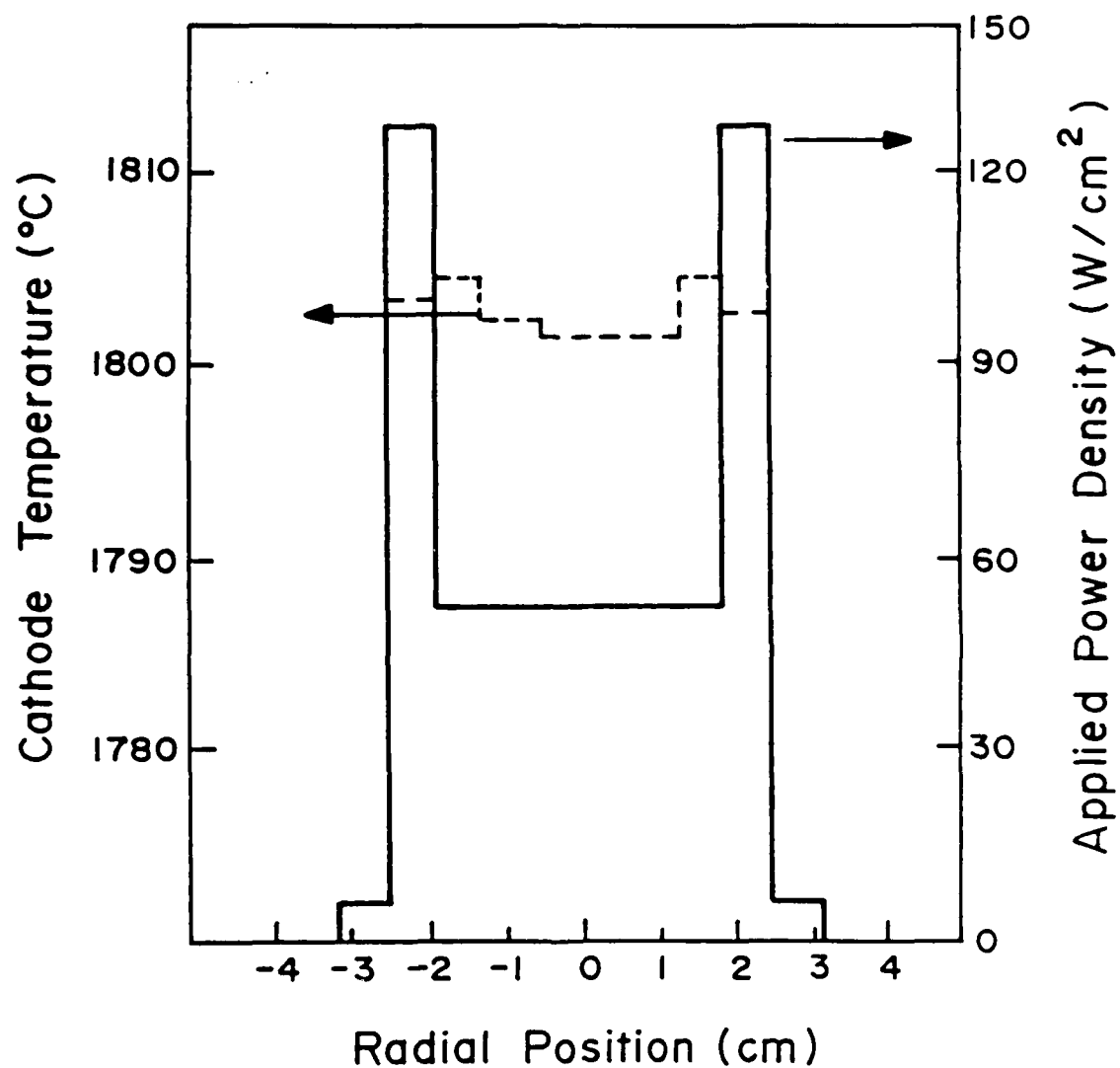and for 50 kV/cm at the cathode surface.

Fig. 2 — Heat loss profile, represented by the solid curve, for a LaB$_6$ cathode heated to 1800°C. The corresponding temperature profile is represented by the dashed curve.
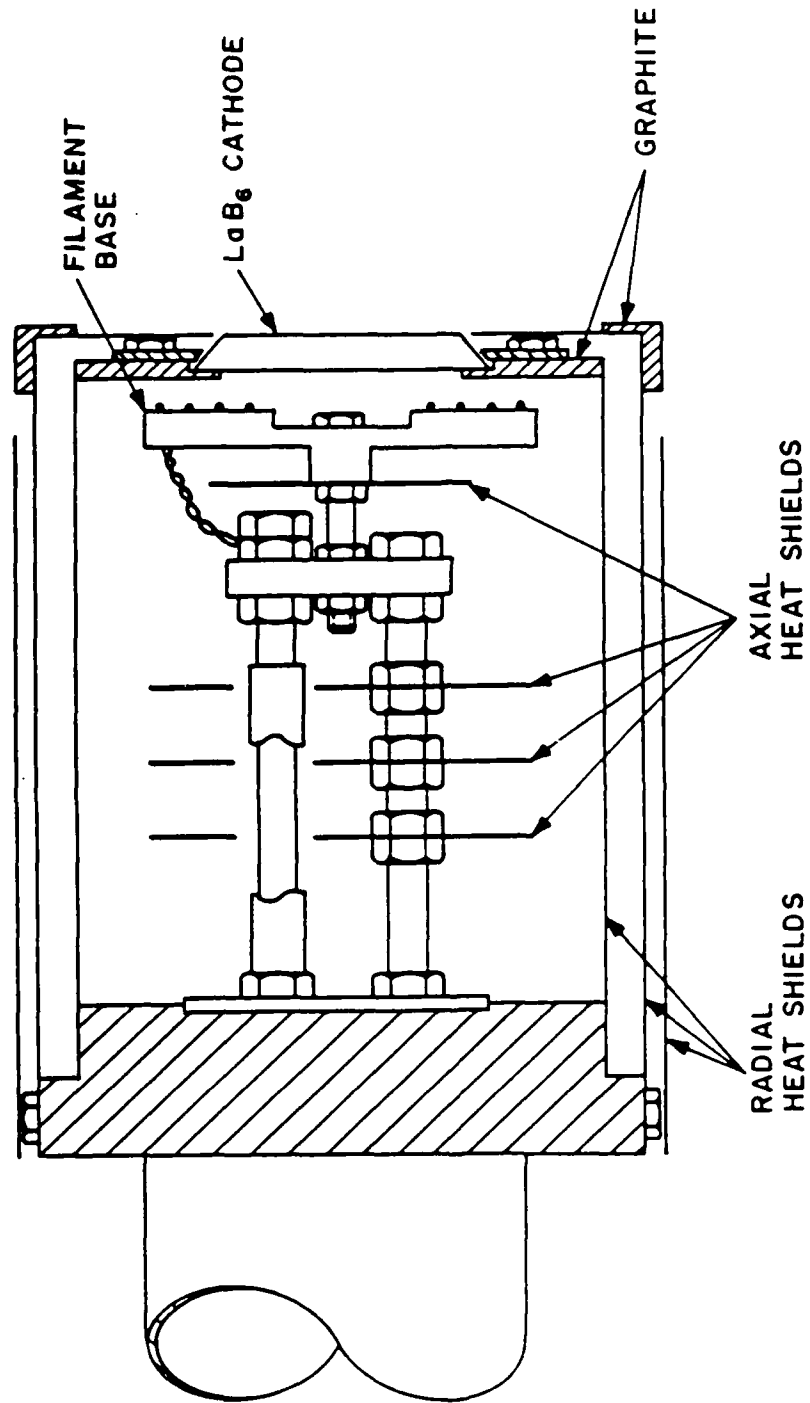
Fig. 3 — Schematic of the cathode heater assembly.

FILAMENT BASE

LaB$_6$ CATHODE
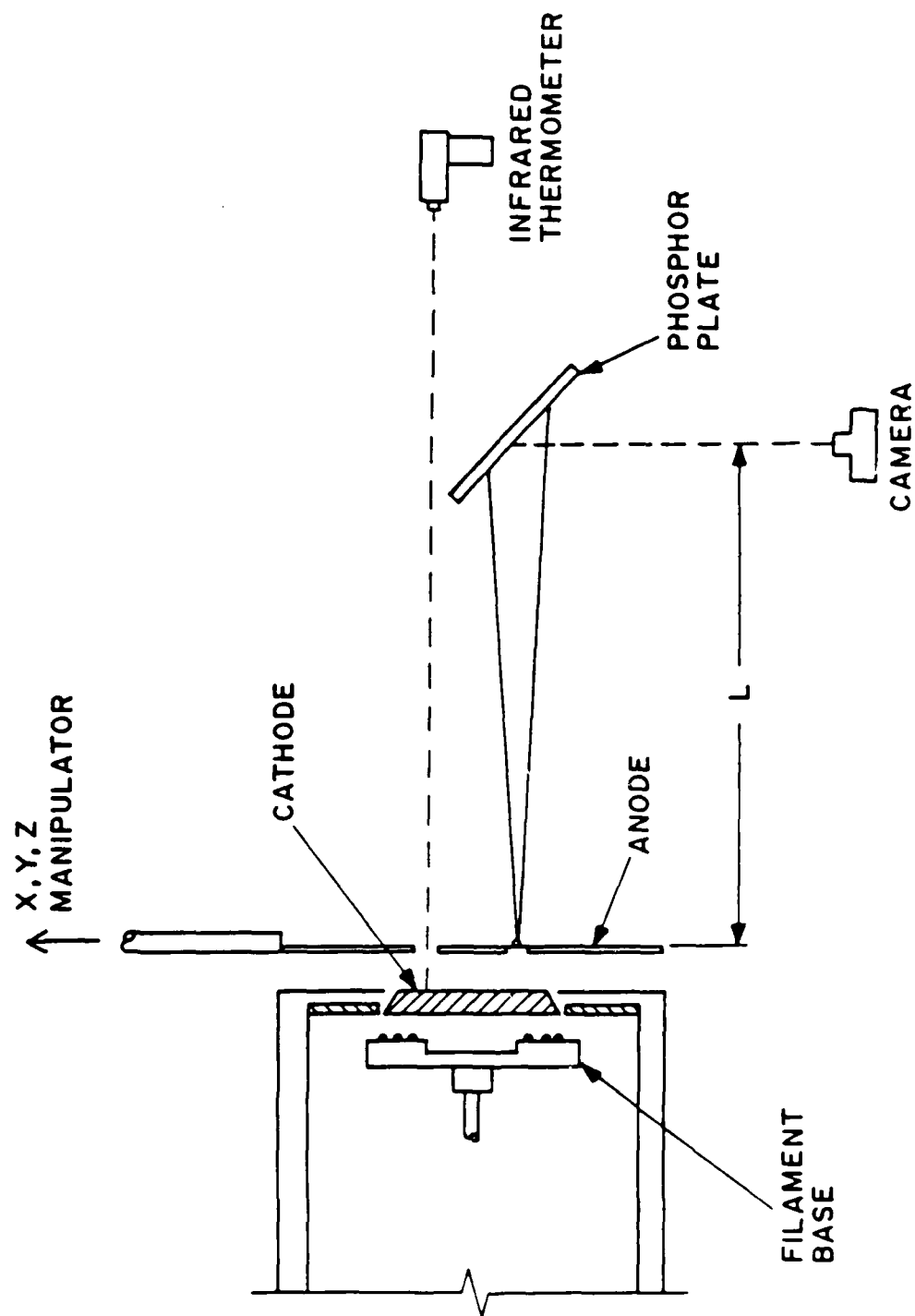
GRAPHITE

AXIAL HEAT SHIELDS

RADIAL HEAT SHIELDS

15

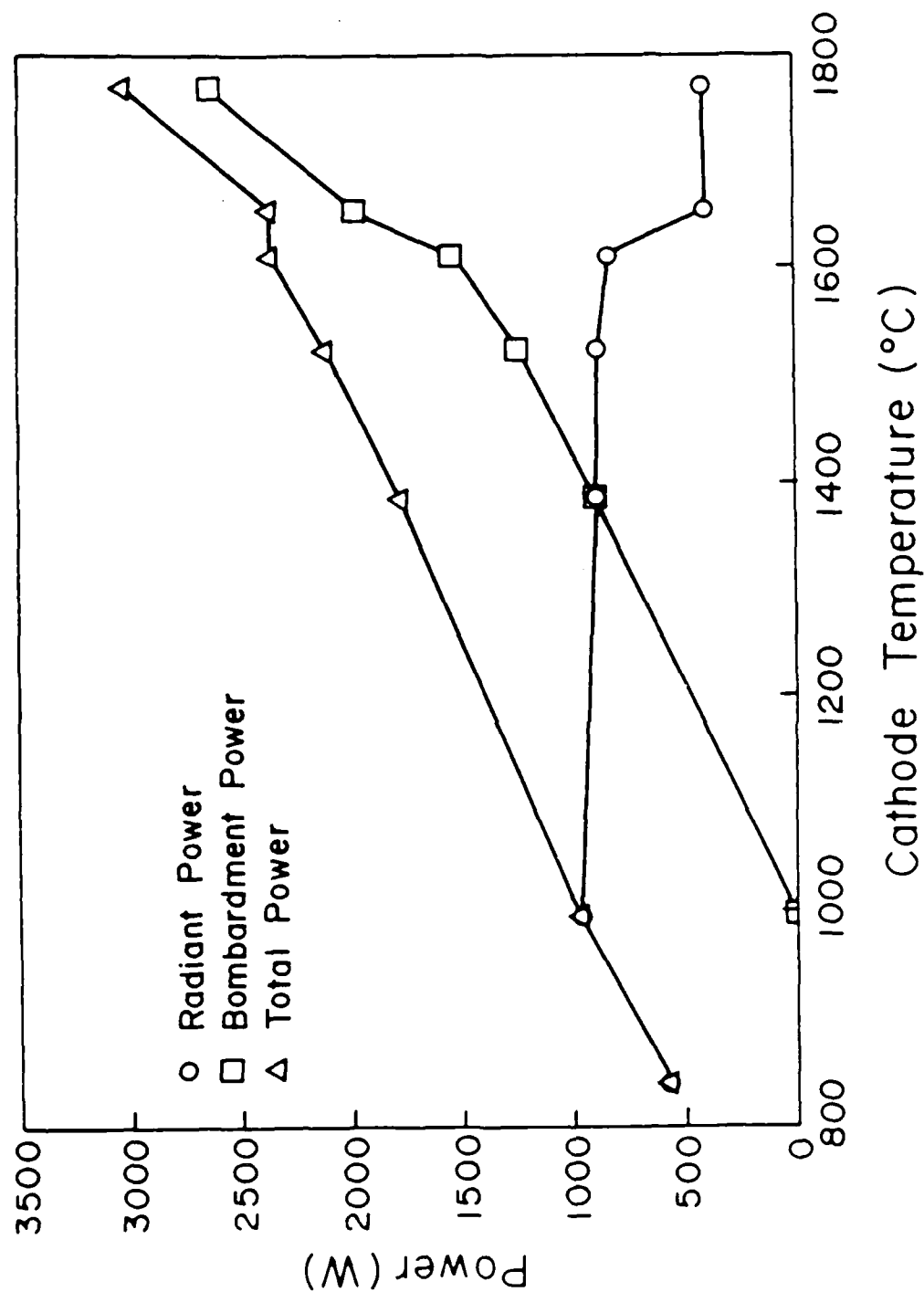Fig. 4 — Schematic of temperature and emittance measurement diagnostics.

Fig. 5 — Measured power levels required to heat a cathode to a given temperature at a fixed reference point, X = 1.3 cm, measured from the cathode center. Data, represented by the discrete symbols, are connected by straight line segments.
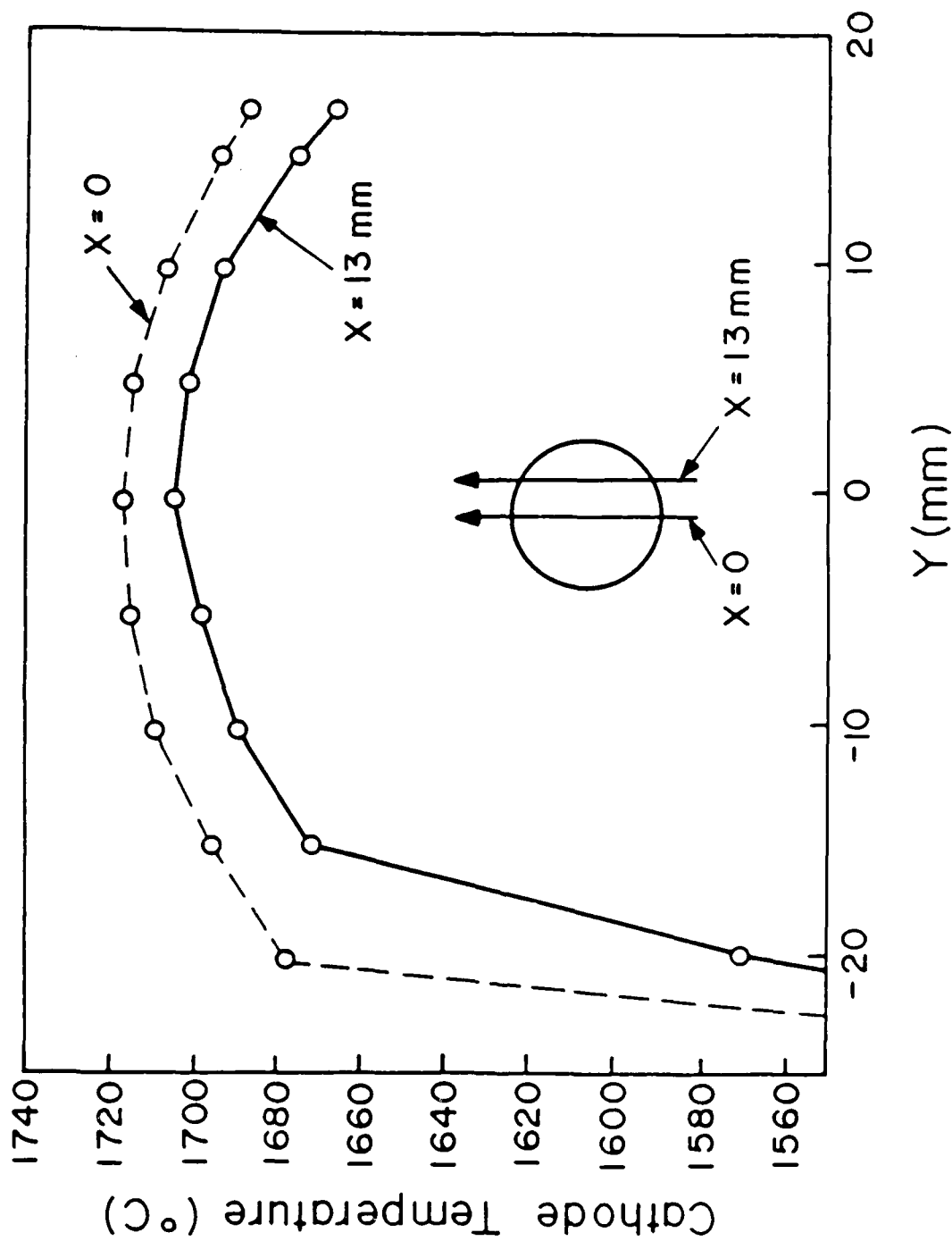
Fig. 6 — Measured cathode temperature profiles as a function of Y for X fixed at 0 mm and 13 mm. Data, represented by the discrete symbols, are connected by straight line segments.
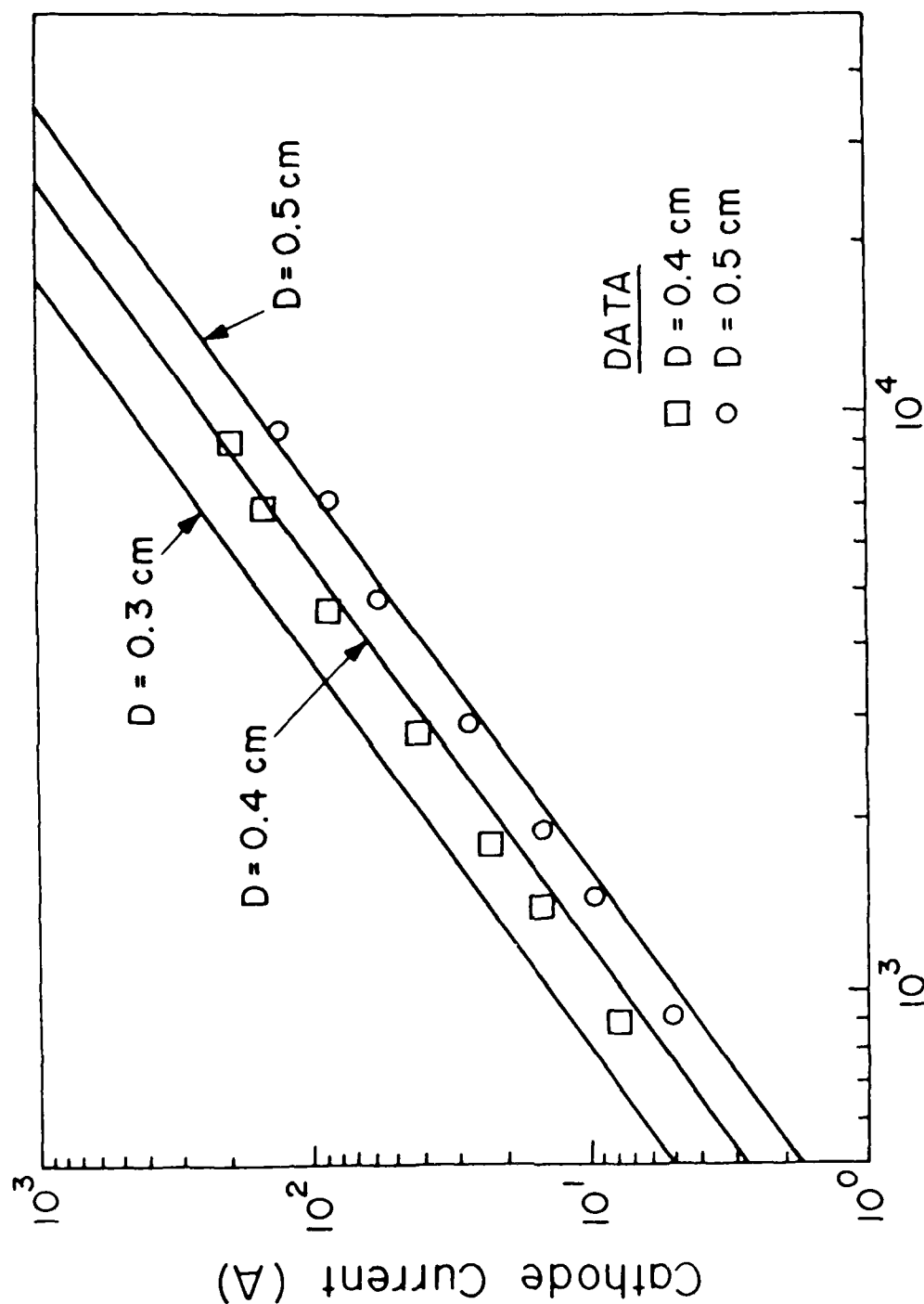
Fig. 7 — Measured value of cathode current as a function of voltage for a 1600°C cathode with cathode-anode gaps at 0.4 cm and 0.5 cm. Data are represented by the discrete symbols. Also shown are straight lines of constant perveance for cathode-anode gaps of 0.3 cm, 0.4 cm, and 0.5 cm.

28 HOURS AT
OPERATING TEMPERATURE

BEFORE OPERATION

Fig. 8 — Electron microscope photographs of LaB$_6$ cathodes. On the left is an unused cathode and on the right is a cathode held at operating temperature for 28 hours.

Dr. M. Allen
Stanford Linear Accelerator Center
Stanford, CA 94305

Dr. W. Barletta
Lawrence Livermore National Laboratory
P.O. Box 808
Livermore, CA 94550

Dr. M. Barton
Brookhaven National Laboratory
Upton, L.I., NY 11101

CDR William F. Bassett
APM for Test Systems Engineering
Naval Sea Systems Command, Code PMS-405
Washington, DC 20362-5101

Dr. Jim Benford
Physics International Co.
2700 Merced St.
San Leandro, CA 94577

Dr. Kenneth Bergerson
Plasma Theory Division - 5241
Sandia National Laboratories
Albuquerque, NM 87115

Dr. Daniel Birx
Lawrence Livermore National Laboratory
P.O. Box 808
Livermore, CA 94550

Dr. Charles Brau
Los Alamos Scientific Laboratory
Los Alamos, NM 87544

Dr. R. Briggs
Lawrence Livermore National Laboratory
P.O. Box 808
Livermore, CA 94550

Dr. Allan Bromborsky
Harry Diamond Laboratory
2800 Powder Mill Road
Adelphi, MD 20783

Dr. H. Lee Buchanan
Lawrence Livermore National Laboratory
P.O. Box 808
Livermore, CA 94550

Dr. M. Butram
Sandia National Laboratory
Albuquerque, NM 87115

Dr. M. Caponi
TRW Advance Tech. Lab.
I Space Park
Redondo Beach, CA 90278

Prof. F. Chen
Department of Electrical Engineering
University of California at Los Angeles
Los Angeles, CA 90024

Dr. D. Chernin
Science Applications Intl. Corp.
1710 Goodridge Drive
McLean, VA 22102

Dr. Charles C. Damm
Lawrence Livermore National Laboratory
P.O. Box 808
Livermore, CA 94550

Prof. R. Davidson
Plasma Fusion Center
M.I.T.
Cambridge, MA 02139

Dr. J. Dawson
University of California at Los Angeles
Department of Physics
Los Angeles, CA 90024

Dr. W.W. Destler
Department of Electrical Engineering
University of Maryland
College Park, MD 20742

Prof. W. Doggett
North Carolina State University
P.O. Box 5342
Raleigh, NC 27650

Dr. H. Dreicer
Director Plasma Physics Division
Los Alamos Scientific Laboratory
Los Alamos, NM 87544

Prof. W.E. Drummond
Austin Research Associates
1901 Rutland Drive
Austin, TX 78758

Dr. J.G. Eden
Department of Electrical Engineering
University of Illinois
155 EEB
Urbana, IL 61801

Dr. A. Faltens
Lawrence Berkeley Laboratory
Berkeley, CA 94720

Dr. T. Fessenden
Lawrence Livermore National Laboratory
P.O. Box 808
Livermore, CA 94550

Dr. A. Fisher
Physics Department
University of California
Irvine, CA 92664

Prof. H.H. Fleischmann
Laboratory for Plasma Studies and
  School of Applied and Eng. Physics
Cornell University
Ithaca, NY 14850

Dr. T. Fowler
Associate Director
Magnetic Fusion Energy
Lawrence Livermore National Laboratory
P.O. Box 808
Livermore, CA 94550

Mr. George B. Frazier, Manager
Pulsed Power Research & Engineering Dept.
2700 Merced St.
P.O. Box 1538
San Leandro, CA 94577

Dr. S. Graybill
Harry Diamond Laboratory
2800 Powder Mill Road
Adelphi, MD 20783

Lt. Col. R. Gullickson
SDIO-DEO
Pentagon
Washington, DC 20301-7100

Dr. J.U. Guillory
JAYCOR
20550 Whiting St., Suite 500
Alexandria, VA 22304

23

Dr. Z.G.T. Guiragossian
TRW Systems and Energy RI/1070
Advanced Technology Lab
1 Space Park
Redondo Beach, CA   90278

Prof. D. Hammer
Laboratory of Plasma Physics
Cornell University
Ithaca, NY   14850

Dr. David Hasti
Sandia National Laboratory
Albuquerque, NM   87115

Dr. C.E. Hollandsworth
Ballistic Research Laboratory
DRDAB - BLB
Aberdeen Proving Ground, MD   21005

Dr. C.M. Huddleston
ORI
1375 Piccard Drive
Rockville, MD   20850

Dr. S. Humphries
University of New Mexico
Albuquerque, NM   87131

Dr. Robert Hunter
9555 Distribution Ave.
Western Research Inc.
San Diego, CA   92121

Dr. J. Hyman
Hughes Research Laboratory
3011 Malibu Canyon Road
Malibu, CA   90265

Prof. H. Ishizuka
Department of Physics
University of California at Irvine
Irvine, CA   92664

Dr. D. Keefe
Lawrence Berkeley Laboratory
Building 50, Rm. 149
One Cyclotron Road
Berkely, CA   94720

Dr. Donald Kerst
University of Wisconsin
Madison, WI 53706

Dr. Edward Knapp
Los Alamos Scientific Laboratory
Los Alamos, NM 87544

Dr. A. Kolb
Maxwell Laboratories
8835 Balboa Ave.
San Diego, CA 92123

Dr. Peter Korn
Maxwell Laboratories
8835 Balboa Ave.
San Diego, CA 92123

Dr. R. Linford
Los Alamos Scientific Laboratory
P.O. Box 1663
Los Alamos, NM 87545

Dr. C.S. Liu
Department of Physics
University of Maryland
College Park, MD

Prof. R.V. Lovelace
School of Applied and Eng. Physics
Cornell University
Ithaca, NY 14853

Dr. S.C. Luckhardt
Plasma Fusion Center
M.I.T.
Cambridge, MA 02139

Dr. John Madey
Physics Department
Stanford University
Stanford, CA 94305

Dr. J.E. Maenchen
Division 1241
Sandia National Lab.
Albuquerque, NM 87511

Prof. T. Marshall
School of Engineering and Applied Science
Plasma Laboratory
S.W. Mudd Bldg.
Columbia University
New York, NY 10027

Dr. M. Mazarakis
Sandia National Laboratory
Albuquerque, NM 87115

Dr. D.A. McArthur
Sandia National Laboratories
Albuquerque, NM 87115

Prof. J.E. McCune
Dept. of Aero. and Astronomy
M.I.T.
77 Massachusetts Ave.
Cambridge, MA 02139

Dr. J. McNally, Jr.
Oak Ridge National Lab.
P.O. Box Y
Oak Ridge, TN 37830

Prof. G.H. Miley, Chairman
Nuclear Engineering Program
214 Nuclear Engineering Lab.
Urbana, IL 61801

Dr. Bruce Miller
Sandia National Laboratory
Albuquerque, NM 87115

Dr. A. Mondelli
Science Applications, Inc.
1710 Goodridge Drive
McLean, VA 22102

Dr. Phillip Morton
Stanford Linear Accelerator Center
Stanford, CA 94305

Dr. M. Nahemow
Westinghouse Electric Corporation
1310 Beutah Rd.
Pittsburg, PA 15235

Prof. J. Nation
Lab. of Plasma Studies
Cornell University
Ithaca, NY 14850

Dr. V.K. Neil
Lawrence Livermore National Laboratory
P.O. Box 808
Livermore, CA 94550

Dr. Gene Nolting
Naval Surface Weapons Center
White Oak Laboratory
10901 New Hampshire Ave.
Silver Spring, MD 20903-5000

Dr. C.L. Olson
Sandia Laboratory
Albuquerque, NM 87115

Dr. Arthur Paul
Lawrence Livermore National Laboratory
P.O. Box 808
Livermore, CA 94550

Dr. S. Penner
National Bureau of Standards
Washington, D.C. 20234

Dr. Jack M. Peterson
Lawrence Berkeley Laboratory
Berkeley, CA 94720

Dr. R. Post
Lawrence Livermore National Lab.
P.O. Box 808
Livermore, CA 94550

Dr. Kenneth Prestwich
Sandia National Laboratory
Albuquerque, NM 87115

Dr. S. Prono
Lawrence Livermore National Lab.
P.O. Box 808
Livermore,. CA 94550

Dr. Sid Putnam
Pulse Science, Inc.
600 McCormick Street
San Leandro, CA 94577

Dr. Louis L. Reginato
Lawrence Livermore National Lab
P.O. Box 808
Livermore, CA 94550

Prof. M. Reiser
Dept. of Physics and Astronomy
University of Maryland
College Park, MD 20742

27

Dr. M.E. Rensink
Lawrence Livermore National Lab
P.O. Box 808
Livermore, CA   94550

Dr. D. Rej
Lab for Plasma Physics
Cornell University
Ithaca, NY   14853

Dr. J.A. Rome
Oak Ridge National Lab
Oak Ridge, TN   37850

Prof. Norman Rostoker
Dept. of Physics
University of California
Irvine, CA   92664

Dr. J. Sazama
Naval Surface Weapons Center
Code 431
White Oak Laboratory
Silver Spring, MD   20910

Prof. George Schmidt
Physics Department
Stevens Institute of Tech.
Hoboken, NJ   07030

Philip E. Serafim
Northeastern University
Boston, MA   02115

Dr. Andrew Sessler
Lawrence Berkeley National Lab
Berkeley, CA   94720

Dr. John Siambis
Lockheed
Palo Alto Research Lab
3257 Hanover Street
Palo Alto, CA   94304

Dr. Adrian C. Smith
Lawrence Livermore National Laboratory
P.O. Box 808
Livermore, CA   94550

Dr. Lloyd Smith
Lawrence Berkeley National Laboratory
Berkeley, CA   94720

Dr. A. Sternlieb
Lawrence Berkely National Laboratory
Berkeley, CA 94720

Dr. D. Straw
W.J. Schafer Assoc.
2000 Randolph Road, S.E., Suite A
Albuquerque, NM 87106

Prof. C. Striffler
Dept. of Electrical Engineering
University of Maryland
College Park, MD 20742

Prof. R. Sudan
Laboratory of Plasma Studies
Cornell University
Ithaca, NY 14850

Dr. W. Tucker
Sandia National Laboratory
Albuquerque, NM 87115

Dr. H. Uhm
Naval Surface Weapons Center
White Oak Laboratory
10901 New Hampshire Ave. Code R41
Silver Spring, MD 20903-5000

Dr. William Weldon
University of Texas
Austin, TX 78758

Dr. Mark Wilson
National Bureau of Standards
Washington, DC 20234

Dr. P. Wilson
Stanford Linear Accelerator Center
Stanford, CA 94305

Prof. C.B. Wharton
303 N. Sunset Drive
Ithaca, NY 14850

West Defense Technical Information Center - 2 copies

NRL Code 2628 - 20 copies

NRL Code 4700 - 26 copies

NRL Code 4710 - 80 copies
NRL Code 1220 - 1 copy

Records 1 copy

Director of Research
U.S. Naval Academy
Annpolis, MD 21402 2 copies

Library
Institut fur Plasmaforschung
Universitat Stuttgart
Pfaffenwaldring 31
7000 Stuttgart 80, West Germany

Ken Takayama
KEN, TRISTAN Division
Oho, Tsukuba, Ibaraki, 305 JAPAN

END

FILMED

FEB. 1988

DTIC